

Preparation and coordinating properties of $\{\text{CH}_2(o\text{-C}_6\text{H}_4\text{CH}_2\text{SbMe}_2)\}_2$, a novel wide-angle *cis*-chelating distibine

Michael D. Brown, William Levason, Gillian Reid* and Michael Webster

Received 27th July 2006, Accepted 3rd October 2006

First published as an Advance Article on the web 16th October 2006

DOI: 10.1039/b610808c

The unique wide-angle distibine, $\{\text{CH}_2(o\text{-C}_6\text{H}_4\text{CH}_2\text{SbMe}_2)\}_2$, **1**, has been prepared indirectly by reaction of Me_2SbCl with the di-Grignard formed unexpectedly by coupling of $o\text{-C}_6\text{H}_4(\text{CH}_2\text{MgCl})_2$ in concentrated thf solution, and directly by treatment of the $\{\text{CH}_2(o\text{-C}_6\text{H}_4\text{CH}_2\text{MgCl})\}_2$ with Me_2SbCl . The very oxygen-sensitive distibine **1** has been characterised by ^1H and $^{13}\text{C}\{^1\text{H}\}$ NMR spectroscopy and high-resolution EIMS. Oxidation of **1** with Br_2 gives the air-stable tetrabromide $\{\text{CH}_2(o\text{-C}_6\text{H}_4\text{CH}_2\text{SbMe}_2\text{Br}_2)\}_2$. Surprisingly, **1** shows a very strong tendency to function as a *cis*-chelate, e.g. to Pt(IV) in the complex $[\text{PtMe}_3\text{I}(\mathbf{1})]$, forming an 11-membered ring and providing a stable Pt(IV) stibine complex, the crystal structure of which shows the Sb–Pt–Sb angle to be $95.96(1)^\circ$. The yellow Pt(II) complex $[\text{PtCl}_2(\mathbf{1})]$ is obtained from reaction of $[\text{PtCl}_2(\text{MeCN})_2]$ with **1** and IR spectroscopic data and a crystal structure determination confirm the Cl ligands are mutually *cis* in this species. Reaction of $[\text{W}(\text{CO})_4(\text{piperidine})_2]$ with **1** in refluxing EtOH gives $[\text{W}(\text{CO})_4(\mathbf{1})]$, the IR spectrum of which shows four $\nu(\text{CO})$ bands, also consistent with *cis*-Sb₂ coordination. The *cis*-chelation is also confirmed by single-crystal X-ray structure determinations of two polymorphs of $[\text{W}(\text{CO})_4(\mathbf{1})]$.

Introduction

In recent years the very elegant work of Werner *et al.* has provided a clear demonstration that the donor properties of stibine ligands are quite distinct from those of phosphine and arsine congeners in organometallic systems, both in promoting different product distributions and providing unprecedented examples of SbR_3 ligands bridging between rhodium centres.^{1,2} Further, within transition metal stibine complexes there is an increased tendency for higher coordination numbers and less M–ER₃ dissociation when E = Sb.^{3,4} Despite these observations there are very few examples of polystibine compounds involving linkages other than saturated, flexible polymethylene units. One of the major constraints in the development of new organostibine ligands is the relative fragility of the C–Sb bonds, the result of which is that fragmentation of these linkages can occur both during the formation of the stibine compounds themselves and upon reaction with certain metal reagents, resulting in substantial decomposition. Furthermore, very little work has been done to probe the effect of the backbone architecture in determining the coordinating properties of distibines.

In our recent work we have used electrophilic reactions of R_2SbCl (R = Me or Ph) with di-Grignard compounds to obtain a series of new distibine ligands incorporating phenylene and xylylene linkages in very good yields, including the *o*-xylyl compound, $o\text{-C}_6\text{H}_4(\text{CH}_2\text{SbMe}_2)_2$.^{5,6} Here we describe the formation and characterisation of the unprecedented wide-angle distibine, **1**, initially obtained as a by-product during such a preparation, and demonstrate its unexpectedly strong tendency to function as a bidentate *cis*-chelate only, to Pt(II) and (IV) and to the $\text{W}(\text{CO})_4$ unit,

despite the length of the linking group between the Sb atoms. Crystal structures of $[\text{PtMe}_3\text{I}(\mathbf{1})]$, $[\text{PtCl}_2(\mathbf{1})]$ and two polymorphs of $[\text{W}(\text{CO})_4(\mathbf{1})]$ are described.

Results and discussion

During the course of our work on the chemistry of $o\text{-C}_6\text{H}_4(\text{CH}_2\text{SbMe}_2)_2$ we have found that this compound may be obtained in very high yield (88%), without the need to distill. However, depending upon the precise conditions employed, the yield is sometimes much lower and its preparation is accompanied by formation of other Sb-containing compounds, including a substantial quantity of Me_4Sb_2 , consistent with a deficit of $o\text{-C}_6\text{H}_4(\text{CH}_2\text{MgCl})_2$. In an effort to probe the identity of the by-products from a lower yielding reaction further, we have investigated the less volatile species obtained by further distillation after fractional distillation of $o\text{-C}_6\text{H}_4(\text{CH}_2\text{SbMe}_2)_2$ *in vacuo* from the reaction mixture. At high temperature (225°C , 0.5 mm Hg), we obtained a colourless, viscous oil. The ^1H NMR spectrum of this shows peaks at similar chemical shifts to the *o*-xylyl distibine, although the CH_2 singlet at 2.96 ppm integrates as 1 : 1 with the *o*-C₆H₄ protons and the aromatic protons and SbMe protons (0.80 ppm) integrate as 2 : 3 (rather than the 1 : 3 ratio expected for $o\text{-C}_6\text{H}_4(\text{CH}_2\text{SbMe}_2)_2$). The accidental coincidence of the SbCH_2 and CH_2CH_2 resonances in this compound was unexpected and initially misleading. However, the $^{13}\text{C}\{^1\text{H}\}$ NMR spectrum shows the expected *o*-C₆H₄ resonances, and the CH_2CH_2 resonances appear as a singlet at 34.9 ppm, while the SbCH_2 and SbMe_2 groups occur at 20.9 and -2.3 ppm respectively—the low frequency resonance arising from the proximity of the heavy Sb atoms. The EIMS shows no evidence for $o\text{-C}_6\text{H}_4(\text{CH}_2\text{SbMe}_2)_2$ (which we have shown previously appears as [parent – Me], $m/z = 393$), but rather the major cluster of peaks is centred at $m/z = 497$,

School of Chemistry, University of Southampton, Highfield, Southampton, UK SO17 1BJ. E-mail: gr@soton.ac.uk; Fax: 023 80593781; Tel: 023 80593609

consistent with loss of Me from the coupled compound $\{\text{CH}_2(o\text{-C}_6\text{H}_4\text{CH}_2\text{SbMe}_2)\}_2$ (**1**). A minor $[\text{parent} + \text{H}]^+$ ion is also evident at $m/z = 513$. The simulated isotope patterns are fully consistent with these assignments and high resolution EIMS confirms the formulation.

Noltes and coworkers have shown previously that the compounds $\text{Me}_2\text{Sb}(\text{CH}_2)_n\text{SbMe}_2$ ($n = 3-6$) undergo redistribution reactions at temperatures in excess of 200°C to eliminate Me_3Sb and give either polymeric species ($n = 3, 6$) or 1-methylstibacycloalkane ($n = 4, 5$).⁷ However, we did not see any evidence for formation of **1** when a sample of $o\text{-C}_6\text{H}_4(\text{CH}_2\text{SbMe}_2)_2$ was heated on the MS probe. Furthermore, no change was observed in the ^1H NMR spectrum of a pure sample of $o\text{-C}_6\text{H}_4(\text{CH}_2\text{SbMe}_2)_2$ after heating to 250°C for 1 h under static vacuum. These results suggest that **1** does not form *via* thermolysis in the fractional distillation.

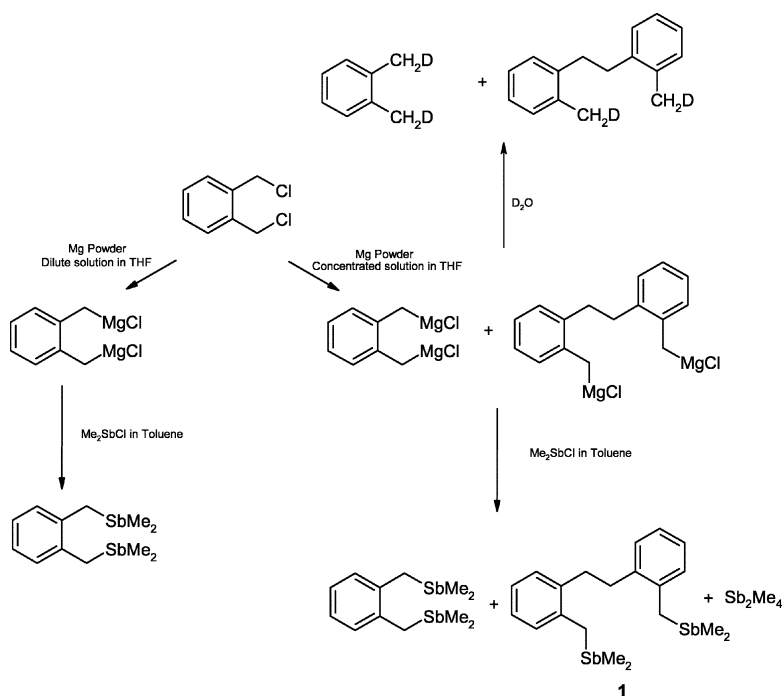
On this basis we concluded that the formation of **1** occurs through partial coupling of the $o\text{-C}_6\text{H}_4(\text{CH}_2\text{MgCl})_2$ di-Grignard in concentrated thf solution. The sensitivity of this di-Grignard to concentration has been noted, and it has been shown to undergo C-C coupling above a critical concentration, also producing bibenzyl species.^{8,9} In order to establish whether this is indeed the source of **1**, $o\text{-C}_6\text{H}_4(\text{CH}_2\text{Cl})_2$ was treated with Mg powder in thf solution and the solution was concentrated *in vacuo* to *ca.* 0.16 mol dm^{-3} and left to stand overnight. D_2O was then added to quench the Grignard, and the organics extracted with Et_2O , dried (MgSO_4) and the solvent removed *in vacuo* to leave a light brown oil (Scheme 1). The ^1H NMR spectrum of this product showed a singlet for the CH_2CH_2 of the coupled ligand backbone at 2.85 ppm and a broad singlet at 2.20 ppm corresponding to (CH_2D) . The presence of the CH_2D groups of $o\text{-C}_6\text{H}_4(\text{CH}_2\text{D})_2$ at 2.14 ppm was also evident. EIMS also showed the only significant species to be $[\{\text{CH}_2(o\text{-C}_6\text{H}_4\text{CH}_2\text{D})\}_2]^+$ ($m/z = 212$) and $o\text{-C}_6\text{H}_4(\text{CH}_2\text{D})_2$ ($m/z = 108$). This result provides strong evidence

that the coupling reaction takes place during formation of the di-Grignard when the concentration of the solution is higher than the 'critical concentration' of 0.075 mol dm^{-3} identified by Lappert *et al.*⁸ As long as the concentration of the solution is maintained below this, the preparation of $o\text{-C}_6\text{H}_4(\text{CH}_2\text{SbMe}_2)_2$ is clean and the yield is very high (routinely $>80\%$).

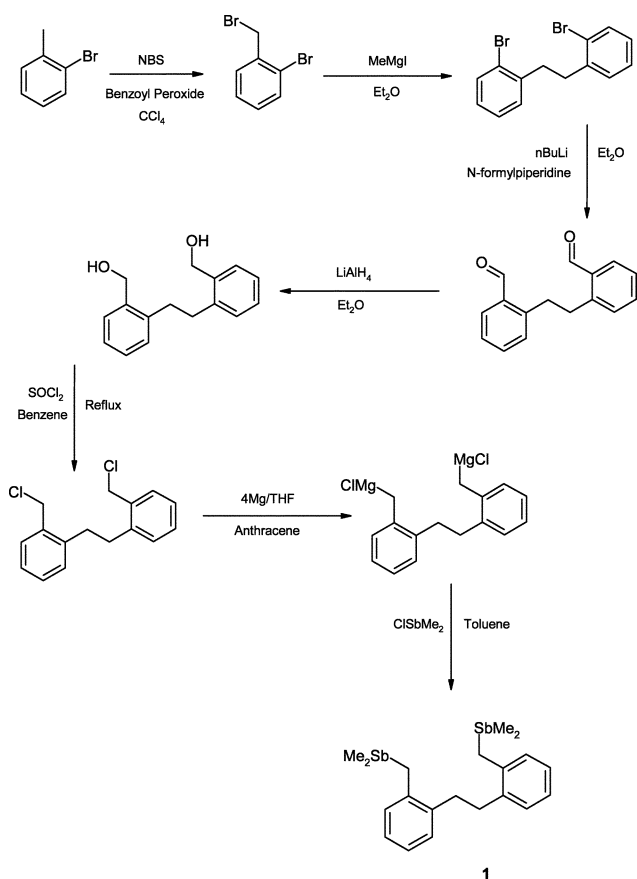
The new distibine **1** was also prepared directly from $\{\text{CH}_2(o\text{-C}_6\text{H}_4\text{CH}_2\text{Cl})\}_2$ (Scheme 2), itself obtained by slight modifications of the literature procedure.¹⁰ Specifically, the conversion of the dialdehyde $\{\text{CH}_2(o\text{-C}_6\text{H}_4\text{CHO})\}_2$ to the diol $\{\text{CH}_2(o\text{-C}_6\text{H}_4\text{CH}_2\text{OH})\}_2$ was achieved in $>90\%$ yield using LiAlH_4 in Et_2O , and the conversion of $\{\text{CH}_2(o\text{-C}_6\text{H}_4\text{CH}_2\text{OH})\}_2$ to $\{\text{CH}_2(o\text{-C}_6\text{H}_4\text{CH}_2\text{Cl})\}_2$ using SOCl_2 required much longer (17 h) reflux to achieve complete conversion. To obtain **1**, the $\{\text{CH}_2(o\text{-C}_6\text{H}_4\text{CH}_2\text{Cl})\}_2$ was then treated overnight with Mg powder and 0.1 mol equiv. of anthracene in thf solution to give the di-Grignard $\{\text{CH}_2(o\text{-C}_6\text{H}_4\text{CH}_2\text{MgCl})\}_2$. Addition of 2 mol equiv. of Me_2SbCl in toluene and subsequent stirring overnight gave **1** as a yellow, air-sensitive oil after work-up. The yield of **1** from this direct synthesis is much higher (68%) than that from the indirect coupling described above. **1** produced by this method was also characterised by ^1H and $^{13}\text{C}\{^1\text{H}\}$ NMR spectroscopy and EIMS and shown to be identical to that obtained as described earlier.

Treatment of **1** with Br_2 gives the tetrabromide of **1** as an air-stable light yellow powder in good yield. The SbCH_2 ($\delta^1\text{H}$: 4.30; $\delta^{13}\text{C}$: 46.33) and SbMe protons ($\delta^1\text{H}$: 2.50; $\delta^{13}\text{C}$: 25.69) which are now bonded directly to the formally $\text{Sb}(v)$ centres are significantly shifted to high frequency *cf.* **1**, whereas, as expected, the bibenzyl CH_2 groups are much less affected ($\delta^1\text{H}$: 3.20; $\delta^{13}\text{C}$: 34.11).

The coordination of long chain diphosphine ligands of the form $\text{R}_2\text{P}(\text{CH}_2)_n\text{PR}_2$ ($n = 6-16$) to transition metals has been studied in detail and shown to give ligand bridged dimers or polymers and occasionally *trans* chelates, but rarely are *cis*-chelates produced



Scheme 1 Formation of **1** *via* coupling of $o\text{-C}_6\text{H}_4(\text{CH}_2\text{MgCl})_2$ in concentrated thf solution.

Scheme 2 Direct synthesis of **1**.

cleanly from such systems.¹¹ However, wide-angle *cis*-chelating phosphines are of considerable current interest owing to the very favourable catalytic properties displayed by their metal complexes, and this has led to major industrial usage.¹² The presence of the two *o*-xylyl substituted units in the backbone of the new distibine **1** led us to speculate on whether **1** has the potential to behave as a wide-angle chelate to metal centres. In order to probe the ligating properties of **1**, one mol equiv. of [PtMe₃I] was reacted with **1** in refluxing CHCl₃ solution under N₂. Following workup, the product [PtMe₃I(**1**)] was isolated as a light yellow solid. Electrospray MS (MeCN) shows clusters of peaks with isotope patterns corresponding to [Pt(**1**)]⁺ (*m/z* = 706), [PtMe(**1**)]⁺ (721) and [PtMe(**1**)(MeCN)]⁺ (762). The ¹H and ¹³C{¹H} NMR spectra confirm the presence of three *fac* Me ligands on Pt, one at very low frequency *trans* to I ($\delta^{13}\text{C}$: -7.8) giving ¹J_{PtC} = 614 Hz and two *trans* to the Sb atoms (6.2 ppm) giving ¹J_{PtC} = 563 Hz. These data are in accord with the other trimethyl-Pt(IV) stibine complexes which we have recently reported.¹³ Two singlet ¹³C{¹H} resonances for the SbMe groups in the coordinated ligand **1** are evident, consistent with the absence of axial symmetry in the [PtMe₃I(**1**)] complex. The ¹⁹⁵Pt NMR spectrum of this complex shows a single resonance at -4440 ppm. This too is in accord with other related stibine complexes of Pt(IV).¹³ These data provide strong support for **1** unexpectedly behaving as a wide-angle *cis*-bidentate on Pt(IV), giving the stable [PtMe₃I(**1**)], containing a very large 11-membered ring.

A single-crystal structure determination on [PtMe₃I(**1**)] provides unambiguous confirmation of the identity of the coupled distibine

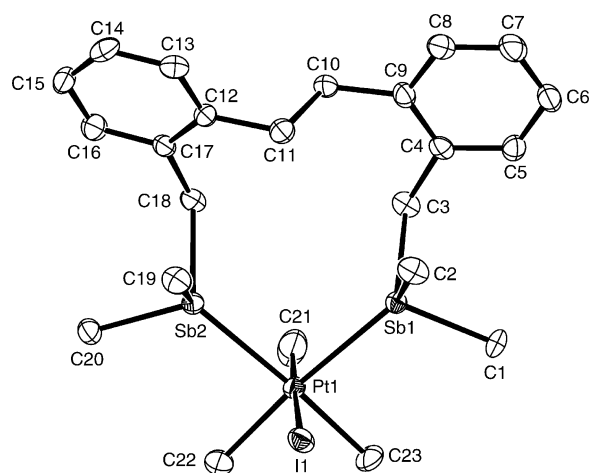


Fig. 1 View of the structure of [PtMe₃I(**1**)] with numbering scheme adopted. Note that there is disorder in the C21–Pt1–I1 region (see Experimental section), the molecule shown is the major component. Ellipsoids are drawn at the 50% probability level and H atoms are omitted for clarity.

Table 1 Selected bond lengths (Å) and angles (°) for [PtMe₃I(**1**)]

Pt1–Sb1	2.6329(4)	Pt1–C22	2.103(5)
Pt1–Sb2	2.6279(4)	Pt1–C23	2.108(5)
Pt1–I1	2.7573(5) ^a	Pt1–C21	2.377(3) ^a
Sb1–C3	2.173(4)	Sb2–C18	2.182(4)
Sb–C(Me)	2.122(5)–2.128(5)	Sb1...Sb2	3.908(1)
Sb1–Pt1–Sb2	95.957(12)	Sb2–Pt1–C22	88.71(15)
Sb1–Pt1–C22	175.09(15)	Sb2–Pt1–C23	174.63(15)
Sb1–Pt1–C23	88.34(15)	Sb2–Pt1–I1	90.83(1) ^a
Sb1–Pt1–I1	87.96(1) ^a	C22–Pt1–C23	87.1(2)
Pt1–Sb1–C3	118.97(13)	Pt1–Sb2–C18	116.53(13)
Sb1–C3–C4	114.1(3)	Sb2–C18–C17	112.4(3)
Pt1–Sb–C(Me)	112.9(1)–121.6(1)	C9–C10–C11–C12	176.1(4)

^a The I1(C21A)–Pt1–C21(I1A) form a disordered group with chemically unreliable bond lengths (see text). The data given are for the major component.

compound and the *cis*-Sb₂ coordination. The structure (Fig. 1, Table 1) shows **1** occupying mutually *cis* coordination sites at a distorted octahedral Pt(IV) centre, with three facial Me ligands and the iodine completing the coordination environment. The Pt–Sb distances are 2.6279(4) and 2.6329(4) Å, slightly longer than in [PtMe₃I{*o*-C₆H₄(CH₂SbMe₂)₂}] (2.6052(4), 2.6204(5) Å)¹³ and substantially longer than in the Pt(II) distibines,⁶ e.g. [PtCl₂{*o*-C₆H₄(CH₂SbMe₂)₂}] (2.4860(7), 2.4931(8) Å) and [Pt{*o*-C₆H₄(CH₂SbMe₂)₂}₂]²⁺ (2.5690(8) to 2.5802(8) Å)—although, of course the higher coordination number in the Pt(IV) species and the strong *trans* influence of the Me groups will both have a significant effect on *d*(Pt–Sb). We also note that the Sb2–Pt1–Sb1 angle in [PtMe₃I(**1**)] is 95.96(1)°, whereas the corresponding Sb–Pt–Sb angle [PtMe₃I{*o*-C₆H₄(CH₂SbMe₂)₂}] is 95.25(1)° and within the more common six-membered chelate rings is < 90°. ¹³

The Pt(II) complex [PtCl₂(**1**)] was obtained in good yield as a yellow solid from reaction of [PtCl₂(MeCN)₂] with **1** in MeCN–CH₂Cl₂ solution. The IR spectrum confirms the presence of mutually *cis* Cl atoms, revealing two ν(PtCl) bands at 316 and 307 cm⁻¹. Platinum-195 NMR spectroscopy shows a single resonance at -4960 ppm, indicative of an Sb₂Cl₂ donor set

at Pt(II).¹⁴ The crystal structure of the yellow [PtCl₂(**1**)] shows (Fig. 2(a) and (b), Table 2) the distibine coordinated to Pt(II) with two mutually *cis* Cl ligands completing the distorted square-planar geometry, $d(\text{Pt-Sb}) = 2.4998(9)$ and 2.5163 \AA , $d(\text{Pt-Cl}) = 2.338(2)$ and $2.350(3) \text{ \AA}$. The chelate angle $\text{Sb1-Pt1-Sb2} = 94.91(3)^\circ$. There is some disorder at the Pt atom – see Experimental

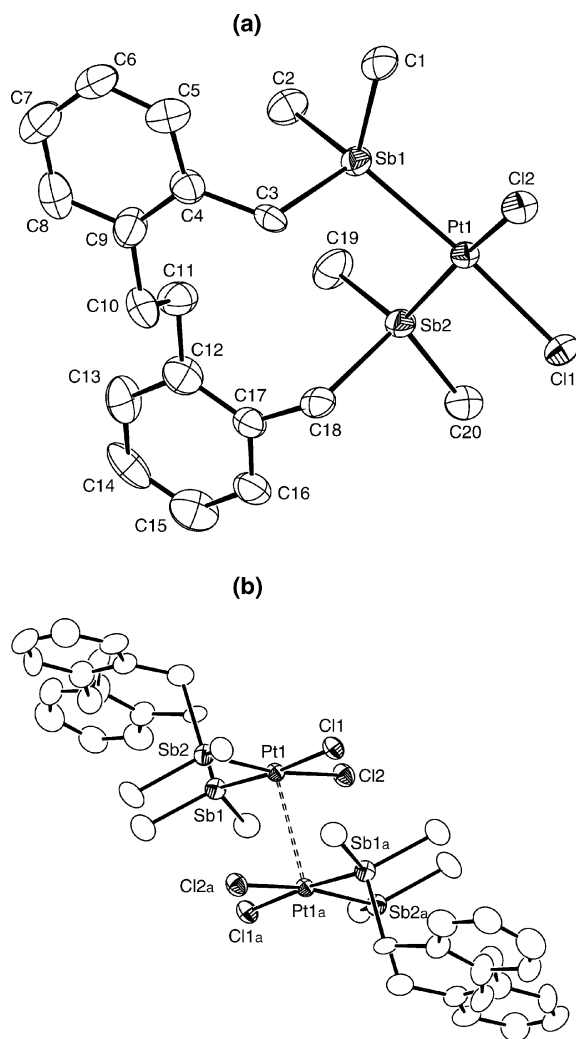


Fig. 2 (a) View of the structure of [PtCl₂(**1**)] with numbering scheme adopted. Note that only the major component of the disorder is shown (see Experimental section). Ellipsoids are drawn at the 45% probability level and H atoms are omitted for clarity. (b) View of the weakly associated, centrosymmetric dimer formed by [PtCl₂(**1**)] (a: $1 - x, -y, 2 - z$).

Table 2 Selected bond lengths (Å) and angles (°) for [PtCl₂(**1**)]

Pt1–Cl1	2.338(2)	Pt1–Cl2	2.350(3)
Pt1–Sb1	2.4998(9)	Pt1–Sb2	2.5163(11)
Pt1...Pt1 ^a	3.1761(12)	Sb1–C1	2.095(10)
Sb1–C2	2.119(10)	Sb1–C3	2.162(10)
Sb2–C20	2.104(10)	Sb2–C19	2.138(10)
Sb2–C18	2.169(11)		
Cl1–Pt1–Cl2	90.48(9)	Cl1–Pt1–Sb1	173.75(7)
Cl2–Pt1–Sb1	87.13(7)	Cl1–Pt1–Sb2	86.63(7)
Cl2–Pt1–Sb2	171.45(7)	Sb1–Pt1–Sb2	94.91(3)

^a $1 - x, -y, 2 - z$.

section, and the discussion refers to the major (91%) component. These compare with $d(\text{Pt-Sb}) = 2.4860(7)$ and $2.4931(8) \text{ \AA}$, $d(\text{Pt-Cl}) = 2.368(3)$, $2.376(3) \text{ \AA}$ and angle $\text{Sb-Pt-Sb} = 97.58(2)^\circ$ in the related species [PtCl₂{*o*-C₆H₄(CH₂SbMe₂)₂}].⁶ The [PtCl₂(**1**)] molecules are distributed across a centre of symmetry such that the planes lie face to face, giving a weakly associated dimer with $d(\text{Pt1} \cdots \text{Pt1a}) = 3.176(1) \text{ \AA}$. This is within the range observed for other weakly associated Pt(II) dimers and chains, e.g. [PtCl₂(H₂NCH₂CH₂NH₂)] $d(\text{Pt} \cdots \text{Pt}) = 3.381(3) \text{ \AA}$.¹⁵

Refluxing a 1 : 1 molar solution of [W(CO)₄(piperidine)₂] and **1** in EtOH gave a light fawn coloured powder following work-up. The Nujol mull IR spectrum of this product shows strong bands in the CO stretching region at 2011, 1898 and a shoulder at 1868 cm⁻¹, indicative of formation of *cis*-[W(CO)₄(**1**)]. These compare with 2012, 1935, 1901 and 1863 cm⁻¹ for *cis*-[W(CO)₄{*o*-C₆H₄(CH₂SbMe₂)₂}] and 2011, 1896 and 1870 for *cis*-[W(CO)₄{Me₂Sb(CH₂)₃SbMe₂}].^{5,16} The APCI MS of this product shows the only significant species is [W(CO)₄(**1**) + H]⁺ ($m/z = 809$) and microanalyses are also consistent with the formulation. Even under prolonged reflux (overnight) in EtOH solution *cis*-[W(CO)₄(**1**)] remains the only significant species. Single crystals of two distinct polymorphs of this compound were obtained from slow evaporation from CH₂Cl₂-Et₂O solutions. The structures show that in each molecule the W(CO)₄ fragment is coordinated to two mutually *cis* Sb atoms of **1** to give a *cis*-chelated distorted octahedral complex. In one of the polymorphs (Fig. 3(a), Table 3) there are two molecules of [W(CO)₄(**1**)] in the asymmetric unit. In one of the two independent molecules the two aromatic rings of the ligand backbone are in the same plane, however, in the second molecule there is some disorder in the backbone of **1**, arising from the presence of two slightly different conformations. The second polymorph shows (Fig. 3(b), Table 3) a very similar species with similar bond length and angle distributions. The W–Sb bond distances lie in the range 2.758–2.774 Å, towards the long end of the range for other stibine complexes with tungsten carbonyl.¹⁷ The Sb–W–Sb chelate angles are in the range 90.34(1)–93.26(1)°. The W–C distances are also sensitive to the *trans* ligand, being significantly longer for $d(\text{W-C}_{\text{trans CO}})$ *cf.* $d(\text{W-C}_{\text{trans Sb}})$, reflecting the modest σ -donor/ π -acceptor properties of the stibine compared to CO.

Conclusions

The new, very air-sensitive distibine, **1**, has been obtained both indirectly and (in high yield) directly from reaction of {CH₂(*o*-C₆H₄CH₂MgCl)}₂ with Me₂SbCl. Incorporation of two *o*-substituted xylene groups within the backbone of **1** plays a very important role in determining its ligating properties. All of our evidence points to **1** functioning as a *cis*-chelate only, giving high yields of the transition metal complexes. Prior to this work, the distibine complexes involving the largest chelate rings were based upon *o*-C₆H₄(CH₂SbMe₂)₂ (seven-membered ring), however, long chain diphosphine ligands with aliphatic linkages, e.g. ¹Bu₂P(CH₂)_{*n*}P¹Bu₂ ($n = 8-10, 12$) and Ph₂P(CH₂)_{*n*}PPh₂ ($n = 6-16$), have been known for many years. These usually produce polymeric, bridged dimeric or occasionally *trans* chelating systems.¹¹ The surprising tendency for *cis*-chelation observed in these complexes of **1** may be due to the *cis*-directing properties

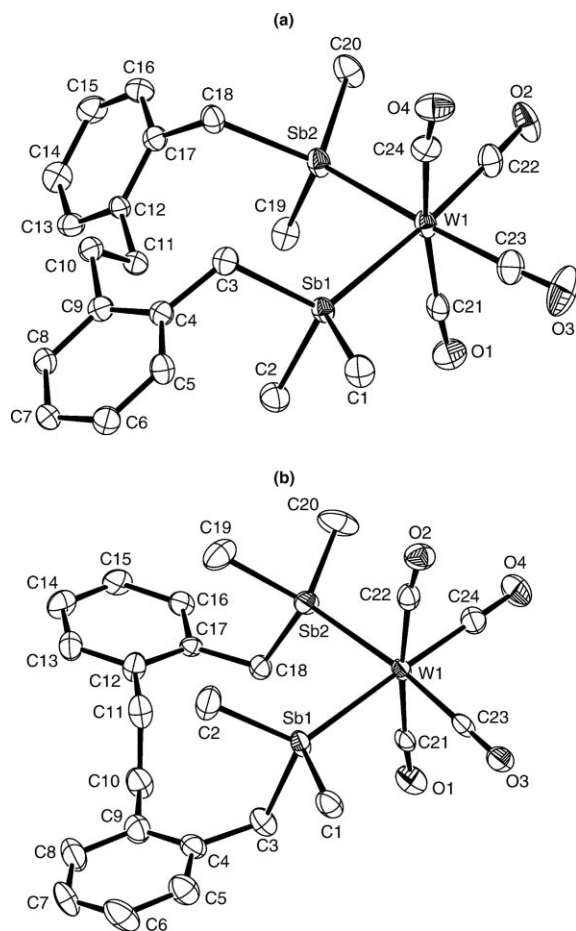


Fig. 3 (a) View of the structure of one of the two crystallographically independent molecules of the first polymorph of $[\text{W}(\text{CO})_4(\mathbf{1})]$ ($P2_1/n$) with numbering scheme adopted. Ellipsoids are drawn at the 50% probability level and H atoms are omitted for clarity. There is some disorder in the ligand backbone in the second molecule—see Experimental section. (b) View of the structure of the second polymorph of $[\text{W}(\text{CO})_4(\mathbf{1})]$ (C_2) with numbering scheme adopted. Ellipsoids are drawn at the 50% probability level and H atoms are omitted for clarity.

conferred by the two *o*-substituted aromatic units in the inter-donor linkage.

Experimental

Infrared spectra were recorded as Nujol mulls between CsI plates using a Perkin-Elmer 983G spectrometer over the range 4000–200 cm^{-1} . Mass spectra were run by electron impact on a VG-70-SE Normal geometry double focusing spectrometer or by positive ion electrospray or APCI (MeCN solution) using a VG Biotech platform. ^1H NMR and $^{13}\text{C}\{^1\text{H}\}$ NMR spectra were recorded using a Bruker AV300 or DPX400 spectrometer (for $^{13}\text{C}\{^1\text{H}\}$ operating at 75.5 or 100.6 MHz respectively) and were referenced to TMS. ^{195}Pt NMR spectra used a Bruker DPX400 spectrometer operating at 85.72 MHz and are referenced to external 1 mol dm^{-3} $\text{Na}_2[\text{PtCl}_6]$ in H_2O . Microanalyses were undertaken by the University of Strathclyde microanalytical service. Solvents were dried prior to use and all preparations were undertaken using standard Schlenk techniques under a N_2

atmosphere. $[\text{PtMe}_3\text{I}]$ and $[\text{W}(\text{CO})_4(\text{piperidine})_2]$ were obtained via the literature methods.^{18,19}

Preparation of 1

Method A. $o\text{-C}_6\text{H}_4(\text{CH}_2\text{MgCl})_2$ was prepared from Mg powder (3.26 g, 134.3 mmol) in thf (150 mL) and $o\text{-C}_6\text{H}_4(\text{CH}_2\text{Cl})_2$ (5.7 g, 32.75 mmol) in thf (50 mL) added dropwise over 1 h giving a 0.16 mol dm^{-3} solution. Me_2SbCl (PhSbMe_2 (15 g, 65.5 mmol) and HCl gas⁵ in toluene (50 mL) was added dropwise over 30 min, and the reaction was left to stir overnight. The mixture was then hydrolysed (100 mL of 1 mol dm^{-3} aqueous NH_4Cl), the organics separated, the aqueous layer extracted with Et_2O (2×50 mL). After drying (MgSO_4), filtering and removing the solvent by distillation at atmospheric pressure, and fractionation of the $o\text{-C}_6\text{H}_4(\text{CH}_2\text{SbMe}_2)_2$ (200 °C, 0.5 mm Hg), **1** was obtained as a clear oil by Kugelrohr distillation (225 °C, 0.5 mm Hg) (yield 1.2 g, 14%). ^1H NMR (CDCl_3): δ 7.1–7.3 (m, 8H, $o\text{-C}_6\text{H}_4$), 2.96 (s, 8H, SbCH_2 , CH_2CH_2), 0.80 (s, 12H, SbMe). $^{13}\text{C}\{^1\text{H}\}$ NMR (CDCl_3): δ 139.9, 138.8, 129.6, 128.5, 126.9, 125.5 ($o\text{-C}_6\text{H}_4$), 34.9 (CH_2CH_2), 20.9 (SbCH_2), -2.3 (SbMe). EIMS: m/z 497 [parent – Me]⁺, 513 [parent + H]⁺. High-resolution MS: calc. for [parent – Me] m/z = 497.00367; found: m/z = 496.9697.

Method B. $\{\text{CH}_2(o\text{-C}_6\text{H}_4\text{CH}_2\text{MgCl})\}_2$ was prepared by adding $\{\text{CH}_2(o\text{-C}_6\text{H}_4\text{CH}_2\text{Cl})\}_2$ (1.6 g, 5.73 mmol) in thf (170 mL) dropwise over 2 h to a flask containing magnesium powder (0.42 g, 17.3 mmol) and anthracene (0.31 g, 1.73 mmol) (which was activated with 1,2-dibromoethane (0.1 mL) in thf (5 mL), and stirred for 5 min). The mixture was stirred at RT overnight, then a solution of Me_2SbCl (prepared from PhSbMe_2 (2.62 g, 11.46 mmol) and HCl gas⁵ in toluene (50 mL) was added dropwise over 2 h, and the resulting mixture stirred at RT overnight. The reaction was hydrolysed with a solution of NH_4Cl (50 mL, 1 mol dm^{-3} in H_2O). The organics were separated and the aqueous layer washed with Et_2O (2×50 mL). The combined organics were then dried over MgSO_4 , filtered and then reduced to dryness. The residues were dissolved in Et_2O (20 mL), the anthracene filtered off, and the pale yellow solution reduced to dryness *in vacuo*. Yellow oil (yield 2.0 g, 68%). ^1H NMR (CDCl_3): δ 7.2–7.0 (m, 8H, $o\text{-C}_6\text{H}_4$), 2.86 (s, 8H, CH_2Sb , CH_2CH_2), 0.80 (s, 12H, SbMe). $^{13}\text{C}\{^1\text{H}\}$ NMR (CDCl_3): δ 139.9, 138.7, 129.6, 128.8, 127.0, 125.5 ($o\text{-C}_6\text{H}_4$), 34.9 (CH_2CH_2), 20.9 (CH_2Sb), -2.3 (SbMe_2). The NMR spectra also show evidence for traces of residual anthracene in the compound. EIMS: m/z 497 [parent – Me]⁺, 513 [parent + H]⁺.

$\{\text{CH}_2(o\text{-C}_6\text{H}_4\text{CH}_2\text{SbMe}_2\text{Br}_2)\}_2$. **1** (0.05 g, 0.098 mmol) was dissolved in dry CH_2Cl_2 (5 mL) and a solution of Br_2 (0.5 mL) and CH_2Cl_2 (10 mL) was added dropwise until a yellow colour was observed. The reaction was then stirred for 2 h, reduced in volume to ca. 2 mL and then hexane (5 mL) was added to precipitate a solid. The light yellow solid was isolated by filtration and dried *in vacuo* (yield 61%). Required for $\text{C}_{20}\text{H}_{28}\text{Br}_4\text{Sb}_2$: C, 28.9; H, 3.4. Found: C, 30.1; H, 3.4% (note that the NMR spectra of this compound and of **1** itself show traces of anthracene from the original direct synthesis of **1** which remain despite repeated washing, hence the poorer than normal fit for the analytical data). ^1H NMR (CDCl_3): δ 7.2–7.4 (m, 8H, $o\text{-C}_6\text{H}_4$), 4.30 (s, 4H, CH_2Sb), 3.20 (s, 4H, CH_2CH_2), 2.50 (s, 12H, Me). $^{13}\text{C}\{^1\text{H}\}$ NMR (CDCl_3):

Table 3 Selected bond lengths (Å) and angles (°) for [W(CO)₄(**1**)]

Polymorph in <i>P2₁/n</i>			
W1–Sb1	2.7736(4)	W2–Sb3	2.7734(4)
W1–Sb2	2.7590(4)	W2–Sb4	2.7589(4)
W1–C21	2.025(5)	W2–C45	2.029(5)
W1–C22	1.968(5)	W2–C46	1.977(5)
W1–C23	1.975(5)	W2–C47	1.980(5)
W1–C24	2.019(5)	W2–C48	2.036(5)
Sb1–C3	2.188(4)	Sb2–C18	2.175(4)
Sb1...Sb2	3.978(1)	Sb3...Sb4	4.022(1)
Sb1–W1–Sb2	91.947(12)	Sb3–W2–Sb4	93.265(12)
C21–W1–Sb1	88.46(11)	C21–W1–Sb2	89.70(12)
C22–W1–Sb1	174.34(13)	C22–W1–Sb2	82.45(13)
C23–W1–Sb1	94.31(14)	C23–W1–Sb2	172.35(14)
C24–W1–Sb1	92.08(12)	C24–W1–Sb2	98.80(13)
C–W1–C (ca. 90°)	85.4(2)–91.2(2)	C24–W1–C21	171.45(18)
W1–Sb1–C3	121.25(11)	W1–Sb2–C18	127.20(11)
Sb1–C3–C4	113.0(3)	Sb2–C18–C17	110.3(3)
C9–C10–C11–C12	174.3(4)		
Polymorph in <i>Cc</i>			
W1–C23	1.966(5)	W1–C24	1.968(5)
W1–C21	2.021(5)	W1–C22	2.041(6)
W1–Sb2	2.7580(4)	W1–Sb1	2.7661(4)
Sb1...Sb2	3.918(1)		
C23–W1–Sb2	174.31(13)	C24–W1–Sb2	89.66(15)
C21–W1–Sb2	87.78(14)	C22–W1–Sb2	95.50(15)
C23–W1–Sb1	85.04(14)	C24–W1–Sb1	177.23(16)
C21–W1–Sb1	88.80(13)	C22–W1–Sb1	96.50(15)
Sb2–W1–Sb1	90.339(14)	C–W1–C (ca. 90°)	88.3(2)–94.8(1)
W1–Sb1–C3	110.85(14)	W1–Sb2–C18	112.45(13)

δ 130.3, 129.5, 129.2, 127.9, 125.7 (*o*-C₆H₄), 46.3 (CH₂Sb), 34.1 (CH₂CH₂), 25.7 (Me).

[PtMe₃I(1**)].** [PtMe₃I] (0.075 g, 0.2 mmol) and **1** (0.102 g, 0.2 mmol) were dissolved in dry CHCl₃ (20 mL) under N₂ and refluxed under N₂ for 4 h. The light yellow solution was then pumped to dryness *in vacuo* to give a waxy solid which was triturated with hexane to produce a light yellow powder (yield 60%). Required for C₂₃H₃₇IPtSb₂·CHCl₃: C, 28.9; H, 3.8. Found: C, 28.2; H, 3.8%. Electrospray MS (MeCN): found *m/z* = 761, 720, 705; calc. for [PtMe(**1**)(MeCN)]⁺ 762, [PtMe(**1**)]⁺ 721, [Pt(**1**)]⁺ 706. ¹H NMR (CDCl₃): δ 0.65 (s, 6H, SbMe), 0.89 (s, 3H, Me *trans* I (²*J*_{PH} = 71 Hz)), 1.16 (s, 6H, SbMe), 1.52 (s, 6H, Me *trans* Sb (²*J*_{PH} = 66 Hz)), 3.10 (s, 4H, CH₂CH₂), 3.28 (m, 4H, SbCH₂), 7.0–7.3 (m, 4H, *o*-C₆H₄). ¹³C{¹H} NMR (CDCl₃): δ -8.5 (2C, SbMe), -7.8 (1C, Me *trans* I (¹*J*_{PC} = 614 Hz)), -5.1 (2C, SbMe), 6.2 (2C, Me *trans* Sb (¹*J*_{PC} = 563 Hz)), 20.5 (2C, SbCH₂), 34.9 (2C, CH₂CH₂), 138.9–124.7 (*o*-C₆H₄). ¹⁹⁵Pt NMR: δ -4440.

[PtCl₂(1**)].** PtCl₂ (0.052 g, 0.195 mmol) was suspended in dry acetonitrile (20 mL) and refluxed for 1 h until all the solid was dissolved and a light yellow solution was obtained. This was then cooled to room temperature, and **1** (0.10 g, 0.195 mmol) in CH₂Cl₂ (5 mL) was added slowly. The reaction mixture was stirred for 2 h at room temperature, until an orange solution was obtained. The solvent was then removed *in vacuo* and the residues were dissolved in a minimum of CH₂Cl₂ and hexane (10 mL) was added to precipitate a solid. The yellow solid was isolated and dried *in vacuo* (yield 55%). Required for C₂₀H₂₈Cl₂PtSb₂·CH₂Cl₂: C, 29.2; H, 3.5. Found: C, 29.0; H, 3.9%. ¹H NMR (CDCl₃): δ 7.0–7.3 (m,

8H, *o*-C₆H₄), 3.36 (s, 4H, CH₂Sb), 2.93 (s, 4H, CH₂CH₂), 1.25 (s, 12H, Me). ¹⁹⁵Pt{¹H} NMR (CH₂Cl₂-CDCl₃): δ -4960. IR (Nujol mull): ν = 316, 307 (ν (PtCl)) cm⁻¹.

[W(CO)₄(1**)].** [W(CO)₄(piperidine)₂] (0.18 g, 0.39 mmol) and **1** (0.20 g, 0.39 mmol) were refluxed in EtOH (20 mL) for 2 h, cooled to RT and the reaction mixture was filtered. The EtOH was removed *in vacuo* and the residues were dissolved in a minimum of CH₂Cl₂. Hexane (10 mL) was added to precipitate a solid, and the light brown powder was isolated and dried *in vacuo* (yield 40%). Required for C₂₄H₂₈O₄Sb₂W: C, 35.7; H, 3.5. Found: C, 35.7; H, 3.5%. ¹H NMR (CDCl₃): δ 7.1–7.4 (m, 8H, *o*-C₆H₄), 3.25 (s, 4H, CH₂Sb), 2.74 (s, 4H, CH₂CH₂), 1.08 (s, 12H, Me). IR (Nujol mull): ν = 2011s, 1898vs, 1868sh (ν (CO)) cm⁻¹. APCI MS (MeCN): *m/z* = 809; calc. for [W(CO)₄(**1** + H)]⁺ 809.

X-Ray crystallography

Details of the crystallographic data collection and refinement parameters are given in Table 4. Yellow single crystals of [PtMe₃I(**1**)], [PtCl₂(**1**)] and two polymorphs of [W(CO)₄(**1**)] were obtained by diffusion of hexane into a CH₂Cl₂ solution, by diffusion of Et₂O into a solution of the complex in CH₂Cl₂ or by slow evaporation from a solution of the complex in CH₂Cl₂-Et₂O, respectively. Data collection used a Nonius Kappa CCD diffractometer (*T* = 120 K) and with graphite-monochromated Mo-K α X-radiation (λ = 0.71073 Å). Structure solution and refinement were routine,^{20–22} except for some disorder between the I and C atoms within the *trans*-I–Pt–Me unit in [PtMe₃I(**1**)]. This was modelled using partial

Table 4 Crystallographic data and refinement details^a

Complex	[PtMe ₃ I(1)]	[PtCl ₂ (1)]	[W(CO) ₄ (1)] (a)	[W(CO) ₄ (1)] (b)
Formula	C ₂₃ H ₃₇ IPtSb ₂	C ₂₀ H ₃₈ Cl ₂ PtSb ₂	C ₂₄ H ₂₈ O ₄ Sb ₂ W	C ₂₄ H ₂₈ O ₄ Sb ₂ W
<i>M</i>	879.02	777.91	807.81	807.81
Crystal system	Monoclinic	Monoclinic	Monoclinic	Monoclinic
Space group	<i>P</i> 2 ₁ / <i>n</i> (no. 14)	<i>P</i> 2 ₁ / <i>c</i> (no. 14)	<i>P</i> 2 ₁ / <i>n</i> (no. 14)	<i>Cc</i> (no. 9)
<i>a</i> /Å	12.2870(15)	14.243(5)	12.9641(15)	17.705(3)
<i>b</i> /Å	12.7061(10)	13.068(3)	23.323(3)	11.6869(15)
<i>c</i> /Å	16.623(2)	12.380(4)	17.0599(15)	12.4991(10)
β /°	91.307(6)	90.302(12)	96.210(5)	94.506(10)
<i>U</i> /Å ³	2594.5(5)	2304.1(12)	5128.0(9)	2578.2(5)
<i>Z</i>	4	4	8	4
μ (Mo-K α)/mm ⁻¹	8.64	8.62	6.59	6.56
<i>R</i> _{int}	0.034	0.148	0.048	0.025
Total no. of obsns.	29152	25377	58518	17199
Unique obsns.	5928	5290	11741	5633
No. parameters	245	240	605	281
<i>R</i> 1 [<i>I</i> _o > 2 σ (<i>I</i> _o)]	0.029	0.057	0.028	0.024
<i>R</i> 1 (all data)	0.036	0.147	0.046	0.025
<i>wR</i> ₂ [<i>I</i> _o > 2 σ (<i>I</i> _o)]	0.062	0.090	0.054	0.049
<i>wR</i> ₂ (all data)	0.064	0.109	0.059	0.049

^a Details in common: *T* = 120 K; λ (Mo-K α) = 0.71073 Å; θ_{\max} = 27.5°. $R_1 = \sum \|F_o\| - |F_c| / \sum \|F_o\|$; $wR_2 = [\sum w(F_o^2 - F_c^2)^2 / \sum wF_o^4]^{1/2}$

atom positions, with the sum of the occupancies of the two I and two C components each being one. Distinct partial C atom and partial I atoms could not be identified, hence these units were refined with identical atomic coordinates and atom displacement parameters. Consequently the Pt–I and Pt–C distances in the *trans*-I–Pt–C unit are weighted averages, and should not be used in comparative studies. The H atoms associated with the disordered Me groups were not included in the final structure factor calculation. The structure of [PtCl₂(1)] shows some disorder in the position of the PtCl₂ fragment. This was evident from a residual unassigned peak in the difference map which based upon the thermal ellipsoids, coordination environment, the distances and angles relative to the Sb₂PtCl₂ plane could not be assigned to a light atom. The disorder model presented gave a very satisfactory refinement for two alternative positions for the Pt atom with relative occupancies of 91 and 9%. This leads to two Sb₂PtCl₂ planes with different orientations, and examination of the centrosymmetric dimer shows that the Cl atoms associated with the minor Pt component and those on the symmetry related Pt1a are common. The discussion and the geometric parameters in Table 2 refer to the major component.

Some disorder was also found in the backbone of one of the two crystallographically independent [W(CO)₄(1)] molecules in the asymmetric unit of the first polymorph (*P*2₁/*n*; (a)). This was modelled very satisfactorily using split C atom occupancies in the disordered region, revealing two slightly different ligand conformations. Selected bond lengths and angles for these species are presented in Tables 1–3.

CCDC reference numbers 285687 and 616260–616262.

For crystallographic data in CIF or other electronic format see DOI: 10.1039/b610808c

Acknowledgements

We thank the EPSRC for support (M. D. B.) and Johnson Matthey plc for loans of platinum metal salts. We also thank Ms Julie Herniman for assistance with the mass spectrometry experiments.

References

- H. Werner, *Angew. Chem., Int. Ed.*, 2004, **43**, 938.
- H. Werner, D. A. Ortmann and O. Gevert, *Chem. Ber.*, 1996, **129**, 411.
- N. R. Champness and W. Levason, *Coord. Chem. Rev.*, 1994, **133**, 115; W. Levason and G. Reid, *Coord. Chem. Rev.*, 2006, **250**, 2565.
- W. Levason and G. Reid, in *Comprehensive Coordination Chemistry II*, ed. J. A. McCleverty and T. J. Meyer, Elsevier, Amsterdam, 2004, vol. 1, p. 377.
- W. Levason, M. L. Matthews, G. Reid and M. Webster, *Dalton Trans.*, 2004, 51.
- W. Levason, M. L. Matthews, G. Reid and M. Webster, *Dalton Trans.*, 2004, 554.
- H. A. Meinema, H. F. Martens and J. G. Noltes, *J. Organomet. Chem.*, 1976, **110**, 183.
- M. F. Lappert, T. R. Martin and C. L. Raston, *Inorg. Synth.*, 1989, **26**, 144.
- M. F. Lappert, T. R. Martin, C. L. Raston, B. W. Skelton and A. H. White, *J. Chem. Soc., Dalton Trans.*, 1982, 1959.
- T. Yamato, N. Sakaue, M. Komine and Y. Nagano, *J. Chem. Res. (S)*, 1997, 246; T. Yamato, N. Sakaue, M. Komine and Y. Nagano, *J. Chem. Res. (M)*, 1997, 1708.
- F. L. March, R. Mason, K. M. Thomas and B. L. Shaw, *J. Chem. Soc., Chem. Commun.*, 1975, 584; A. J. Pryde, B. L. Shaw and B. Weeks, *J. Chem. Soc., Chem. Commun.*, 1973, 947; F. L. March, R. Mason, K. M. Thomas and B. L. Shaw, *J. Chem. Soc., Dalton Trans.*, 1976, 322; W. E. Hill, D. M. A. Minehan, J. C. Taylor and C. A. McAuliffe, *J. Am. Chem. Soc.*, 1982, **104**, 6001; B. L. Shaw, *J. Organomet. Chem.*, 1980, **200**, 307.
- P. W. N. M. van Leeuwen, P. C. J. Kamer, J. N. H. Reek and P. Dierkes, *Chem. Rev.*, 2000, **100**, 2741, and references therein.
- M. D. Brown, W. Levason, G. Reid and M. Webster, *Dalton Trans.*, 2006, 1667.
- E. G. Hope, W. Levason and N. A. Powell, *Inorg. Chim. Acta*, 1986, **115**, 187.
- J. Iball, M. MacDougall and S. Scrimgeour, *Acta Crystallogr., Sect. B*, 1975, **31**, 1672.
- M. D. Brown, W. Levason, J. M. Manning and G. Reid, *J. Organomet. Chem.*, 2005, **690**, 1540.
- A. M. Hill, N. J. Holmes, A. R. J. Genge, W. Levason, M. Webster and S. Rutschow, *J. Chem. Soc., Dalton Trans.*, 1998, 825.
- J. C. Baldwin and W. C. Kaska, *Inorg. Chem.*, 1975, **14**, 2020.
- D. J. Darensbourg and R. L. Kump, *Inorg. Chem.*, 1978, **17**, 2680.
- G. M. Sheldrick, *SHELXS-97, program for crystal structure solution*, University of Göttingen, Germany, 1997.
- G. M. Sheldrick, *SHELXL-97, program for crystal structure refinement*, University of Göttingen, Germany, 1997.
- H. D. Flack, *Acta Crystallogr., Sect. A*, 1983, **39**, 876.